

Received April 17, 2020, accepted April 30, 2020, date of publication May 4, 2020, date of current version May 19, 2020.

Digital Object Identifier 10.1109/ACCESS.2020.2992313

# Multi-State Circularly Polarized Antenna Based on the Polarization Conversion Metasurface With Gain Enhancement

## TING WU<sup>10</sup>, JUAN CHEN, AND MING-JUN WANG

Xi'an University of Technology, Xi'an 710048, China

Corresponding author: Ting Wu (wutingzdh@xaut.edu.cn)

This work was supported in part by the Program for Talent of Colleges and Universities Service Enterprise of Xi'an under Grant 201805037YD15CG21(10), in part by the Program for Science and Technology Innovation of Xi'an University of Technology under Grant 103-451117003, in part by the Xi'an Beilin District Science and Technology Plan under Grant GX1920, in part by the Natural Science Foundation of Shaanxi under Grant 2020JQ-653, in part by the Foundation of Key Laboratory of Antenna and Microwave Technology under Grant 61424020508192402013, and in part by the Foundation of Educational Commission of Shaanxi Province under Grant 18JK0561.

**ABSTRACT** In this paper, a multi-state circularly polarized antenna with gain enhancement is proposed based on the polarization conversion metasurface(PCM). The antenna is composed of a simple monopole antenna and a modified PCM coating which is made up of a series of arrow-shaped elements distributed partly on the back of the substrate. The dimension of the antenna is  $42 \times 43$ mm. And Genetic Algorithm (GA) is adopted to obtain the best performance of the PCM. The coating is used as a reflector, compared with the radiating wave, the amplitude of the reflected wave is equal and the phase is  $90^{\circ}$  difference. Therefore, circularly polarized antenna is obtained with a low profile. By rotating the orientation of the element, the antenna changes from LHCP to RHCP which means the antenna can work in multi-state. In addition, the gain of the antenna is improved. Both of the simulated and measured results have verified the design. The simulated and measured results show that the operating band of the proposed CP radiation is 10.2 to 10.9 GHz. And the gain is improved for 1 dB in average with the peak being 2 dB at 10.9 GHz.

**INDEX TERMS** Polarization conversion, multi-state, metasurface, genetic algorithm, circularly polarized, gain enhancement.

### I. INTRODUCTION

With the speed development of wireless communications, circularly polarized (CP) antennas have drawn more and more attention due to their advantages in improving the polarization efficiency. Circularly polarized antennas are prominent in communication systems due to the flexibility in the arrangement of antennas at both trans-receiver side and also reduce the losses occurring due to the Faraday rotation effects [1]. On the other hand, a CP antenna is advantageous for the positional freedom of the receiver [2], [3]. In recent years, metasurface antennas have been used to reduce the antenna profile [4], enlarge the operating band [5], [6], full-space wave control [7], [8] and improve the directivity of the antenna [9], [10]. The researchers can convert a linearly polarized wave into the cross-polarized one to achieve the

The associate editor coordinating the review of this manuscript and approving it for publication was Kwok L. Chung.

multi-function. In [11], the authors proposed a metasurface combined with a microstrip antenna to convert LP to CP signals. A combination of an microstrip antenna array with metasurface was proposed in [12]. The structure obtained an AR BW bigger than 200 MHz, but the structure was large and very complex. The polarization conversion metasurface (PCM) is a kind of artificial surface that can effectively convert a linearly polarized wave into the cross-polarized one [13]–[18]. In recent decades, various antennas based on PCM have been widely researched. CP waves can be generated by the polarization conversion metasurface [19]. In [20], the polarization conversion ratio of the proposed double V-shaped PCM could reach more than 90%. In [21], the polarization conversion ratio of the proposed fishbone-shaped PCM could reach more than 50% with the relative bandwidth of 103.6%. However the structures of these antennas are somewhat complicated and are not very available for actual uses.

In this letter, a low profile and high gain circularly polarized antenna based on PCM structure is proposed. We adopt the genetic algorithm (GA) to obtain the best performance of the antenna [22], [23]. By rotating the orientation of the element, the antenna changes from LHCP to RHCP which shows the polarization reverse characteristic. This means the antenna can work in multi-state and provides a great freedom for the practical application. The proposed antenna is fabricated to verify the design. From the simulated and measured results, we can see that the operating bandwidth of the CP radiation can reach 10.2 to 10.9 GHz. Meanwhile, the gain of the proposed antenna has been improved for more than 1 dB in the operating band. Moreover, the antenna is both simple in design and fabrication which demonstrate the suitability for the actual uses. The paper includes five parts. First, we discuss the design and optimization of the proposed antenna in section II. And then, the experimental results and discussion are presented in section III. Finally, the work is concluded in section IV.

# II. DESIGN AND OPTIMIZATION OF THE PROPOSED ANTENNA

### A. STRUCTURE AND EVOLUTION OF THE ELEMENT

Figure 1 shows the structure of the proposed PCM element which is composed of two T-shaped patches placed along the diagonals of the rectangle. The element is printed on an FR4 substrate with a thickness of  $H_1=0.8$  mm, relative permittivity of  $\varepsilon_r=4.4$ , and loss tangent of 0.02. The geometry sizes of the element are as follows: A=7 mm, H=2.1 mm,  $W_3=1$  mm,  $W_4=0.2$  mm,  $L_7=4.1$  mm,  $L_8=1.8$  mm. The high-frequency structure simulator (ANSYS HFSS 13.0) is used to simulate and study the antenna structure.

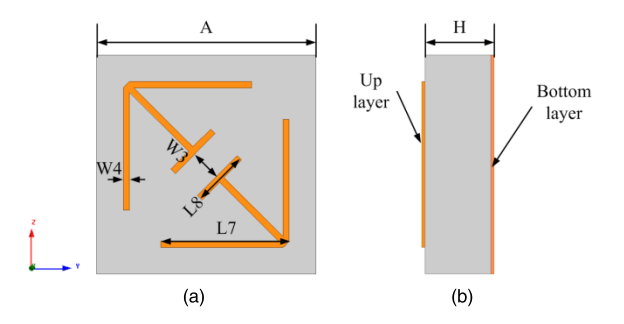
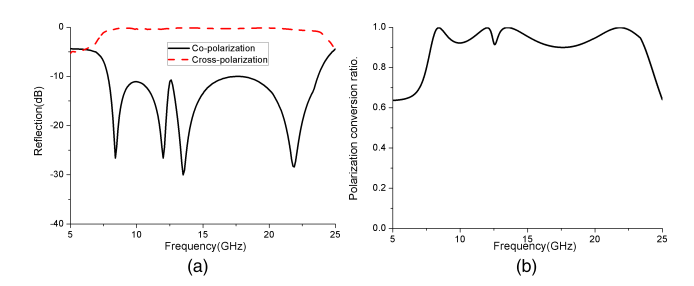


FIGURE 1. Configuration of the proposed element. (a) Top view (b) Side view.

The simulated reflection coefficient and polarization conversion ratio of the proposed PCM element are given in Figure 2 (a) and (b) respectively. It can be seen that the operating band of the PCM element is ranging from 7.83-23.69GHz with the condition of reflection coefficient less than -10 dB. In Figure 2 (b), we can see that the operating band is ranging from 11.5GHz to 22.0GHz with the PCR greater than 90%. This curve means that in the operating band, more than 90% of the linearly polarized incident power can be converted into its cross-polarized power.

Figure 3 shows the relatively reflected phase curves of the proposed element (designed unit cell) and PEC.



**FIGURE 2.** Simulated performances of the proposed PCM. (a) Reflection coefficient. (b) Polarization conversion ratio.

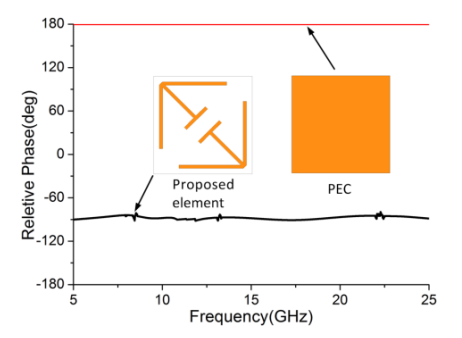


FIGURE 3. Relative reflection phase of the proposed element.

From the given curves, we can clearly see that when the plane is illuminated by a 0° relative phase incident wave, a nearly  $-90^{\circ}$  relative reflected phase can be obtained on the proposed element. And a 180° relative reflected phase can be obtained on the PEC. The relatively reflected phase curve of PEC is constant while that of proposed element is changing with a minor variation. To better understand the mechanism and design process, the evolution of the PCM element and the simulated reflection coefficient of the elements are given in Figure 4 and Figure 5. It can be seen that the reflection coefficient of the simple rectangle element is narrow. And then, the rectangle is modified by adding two branch along the diagonals. By this way, we can see that the high frequency resonance at about 23 GHz is introduced. At last, the branch is replaced by a T-shaped patch to reduce the reflection at 19 GHz. And the proposed element shows good UWB performance.

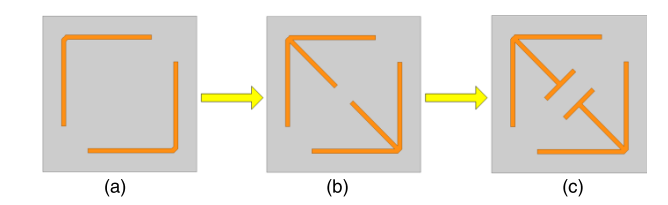


FIGURE 4. Evolution of the proposed element. (a) Rectangle element (b) Modified rectangle element (c) Proposed element.

# B. PARAMETRIC STUDY AND OPTIMIZSATION ALGORITHM

To choose the best parameters, we change one parameter at a time while keeping the other parameters unchanged to observe the influence. First, the effects of different length of

VOLUME 8, 2020 84661



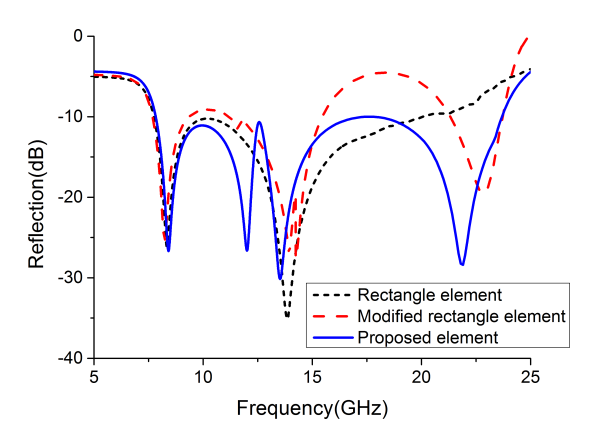


FIGURE 5. Reflection coefficient of the elements.

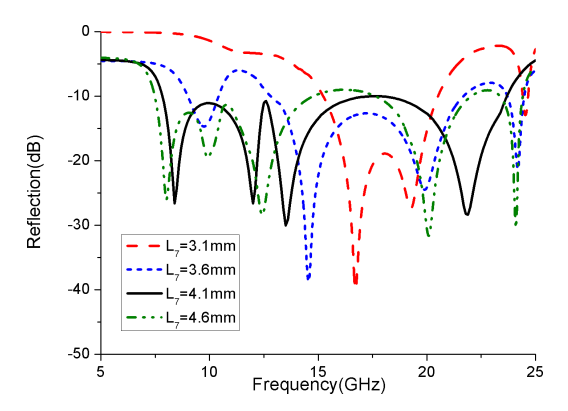


FIGURE 6. Effect of L<sub>7</sub> on the proposed element performance.

L<sub>7</sub> on the reflection coefficient are shown in Figure 6. L<sub>7</sub> is the side length of the square cell, which we change from 3.1 to 4.6 mm. It can be seen that the higher operating band decreases as the L<sub>7</sub> increases. Meanwhile the performance of the lower operating band is affected. For balance, we chose  $L_7 = 4.1$  mm. In Figure 7, we can see that the width of the square cell side length W4 has influence on the higher operating band, and the performance of the higher operating band becomes worse as W<sub>4</sub> increases. Taking into account the lower operating band,  $W_4 = 0.2$  mm is chosen. As shown in Figure 8, the performance of the higher operating band becomes better as the  $L_8$  increases. When  $L_8 = 1.8$  mm, the element has the widest lower impedance bandwidth. Thus, in this paper, we set  $L_8 = 1.8$  mm. Then, the effects of different gap widths W<sub>3</sub> are studied. As shown in Figure 9, the influence of W<sub>3</sub> is focus on the lower frequency band, while the higher operating band is almost unchanged.

In the above discussion, only one parameter is changed while keeping the other parameters unchanged. By this means, the influence of the different parameters can be studied independently. Also an approximate solution for the optimized parameter is found. However, all the parameters can be adjusted and optimized simultaneously to obtain the global optimum of the element. Thus, genetic algorithm (GA) is adopted to obtain the best performance of the PCM. We use the GA tool in MATLAB software with the tournament selection strategy. The value calculated by the full-wave

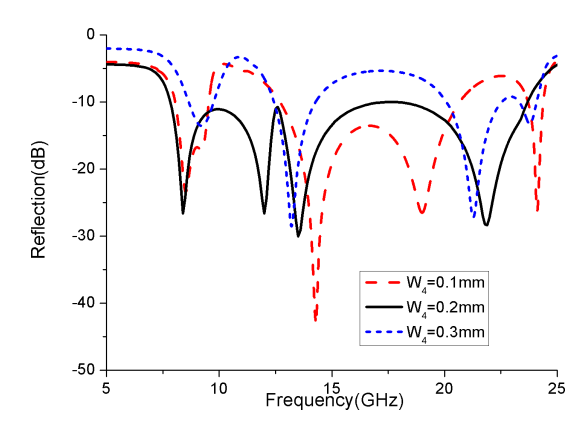


FIGURE 7. Effect of W<sub>4</sub> on the proposed element performance.

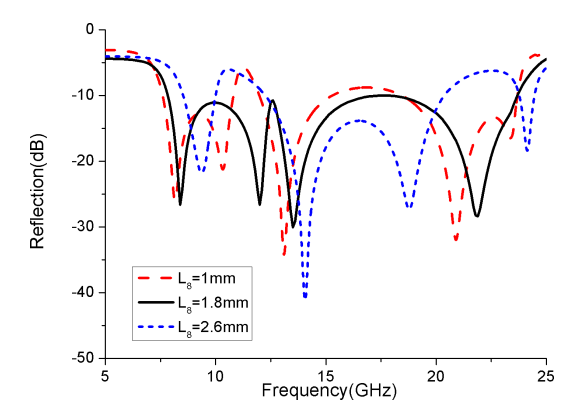


FIGURE 8. Effect of L<sub>8</sub> on the proposed element performance.

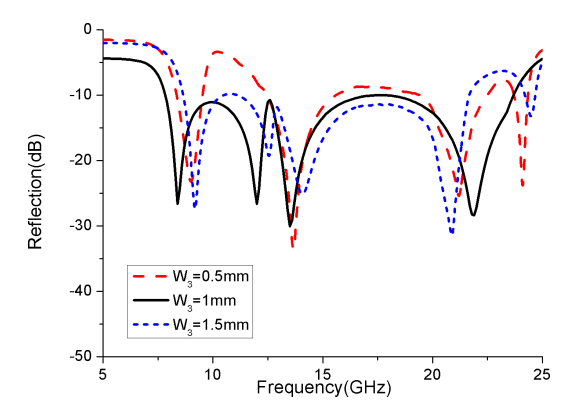


FIGURE 9. Effect of W<sub>3</sub> on the proposed element performance.

electromagnetic simulation software HFSS is taken in each iteration of the fitness function.

Some parameters such as the side length of the square cell  $L_7$ , the length of the T-shape stub  $L_8$ , and the gap width  $W_3$  need to be optimized. A multi objective optimization is required if we want to obtain a good reflection coefficients bandwidth. The fitness function consists of the reflection coefficients bandwidth ( $S_{11.BW}$ ) as follows:

$$fitness\_function = 1 - w_1 S_{11.BW}$$
 (1)

with

$$S_{11.BW} = \frac{2(f_{p2} - f_{p1})}{f_{p2} + f_{p1}} \tag{2}$$

84662 VOLUME 8, 2020



in which  $f_{p2}$  and  $f_{p1}$  are the higher and lower frequencies, respectively.  $|S_{11}| = -12dB$ ,  $w_1 = 0.5$ . A more rigorous condition of  $|S_{11}| = -12dB$  instead of  $|S_{11}| = -10dB$  is used to improve the resonance of the element better. The fitness function should to be positive and minimum to obtain the widest bandwidth. Table 1 shows the other parameters used in the GA algorithm. And the optimized geometrical parameters are as follows:  $W_3 = 1$  mm,  $L_7 = 4.1$  mm and  $L_8 = 1.8$  mm. After the optimization, the return loss bandwidth of the proposed PCM is 100.6% ranging from 7.83-23.69 GHz.

**TABLE 1.** Parameters used in the GA optimization.

GA parameter	Value		
Population size	200		
Number of generations	100		
Selection mechanism	Tournament		
Cross rate	90%		
Mutation rate	10%		
Optimization goals	(1)Maximize		
	the impedance		
	bandwidth		
	$ S_{11}  = -12dB$ ;		
	(2) Maximize		
	the 3-dB gain		
	bandwidth		

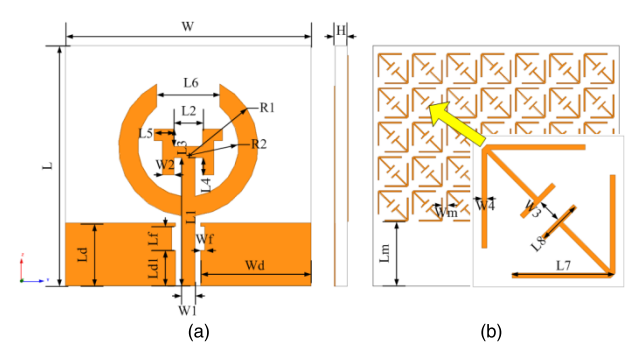


FIGURE 10. The structure of the antenna. (a) Top view (b) Back view.

## C. ANTENNA STRUCTURE

The structure of the proposed antenna is shown in Figure 10. The antenna is simply composed of a monopole antenna which is protruded into round to achieve efficient excitation and a modified PCM coating. And the coating which is made up of a series of proposed PCM elements is etched on the back of the substrate partly. The PCM array is formed by  $5 \times 7$  elements uniformly distributed along the x and y directions, with a gap width Wm. The antenna is printed on a single-layer FR4 substrate with  $\varepsilon_r = 4.4$ , loss tangent of 0.02, and thickness of 2.1mm. The optimized dimension of the antenna are listed in Table 2.

To better understand the effect of the PCM coating and the reason of the gain enhancement, the simulated reflection

TABLE 2. Parameters for the proposed antenna (Unit: mm).

L	W	Н	$L_1$	$L_2$	$L_3$
42	43	2.1	22.4	5	3
$L_4$	$L_5$	$L_6$	$L_7$	$L_8$	$L_d$
3	3.5	11	4.1	1.8	11
$L_{d1}$	$L_{\rm f}$	$L_{\rm m}$	$\mathbf{W}_1$	$W_2$	$W_3$
6.2	4.2	11.35	2.4	2	1
$W_4$	$W_d$	$W_{\rm f}$	W <sub>m</sub>	$R_1$	$R_2$
0.2	19.3	0.7	0.7	12.2	8.8

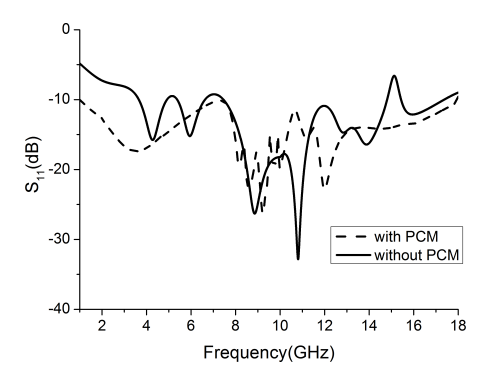


FIGURE 11. Simulated reflection coefficient of the antennas with and without PCM.

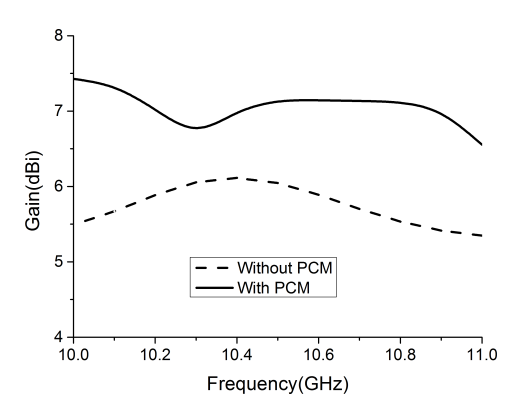
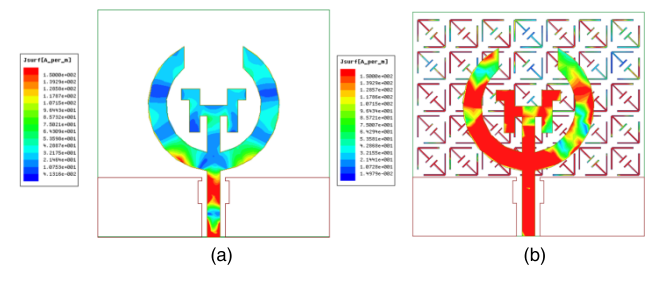


FIGURE 12. Simulated gain of the antennas with and without PCM.



**FIGURE 13.** The surface current distribution of the antennas. (a) without PCM (b) with PCM.

coefficient and gain of monopole antennas with and without PCM are shown in Figure 11 and Figure 12 respectively. Figure 13 shows the simulated surface current distribution of the monopole antennas without and with PCM at 10.6 GHz. We can see the induced current excited by the monopole antenna on the PCM elements is stronger compared with that

VOLUME 8, 2020 84663



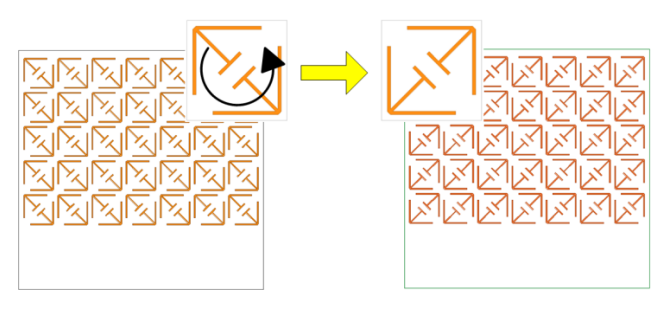


FIGURE 14. Structure of the proposed and reverse antennas.

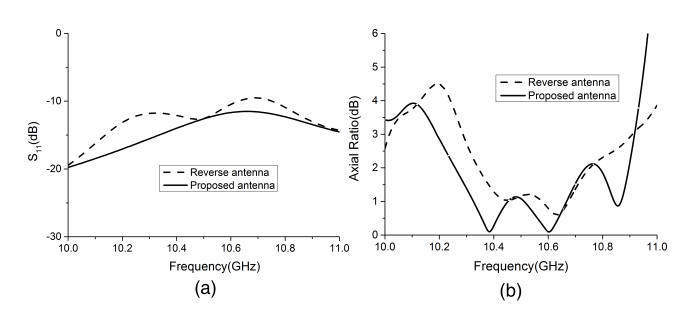


FIGURE 15. Simulated performance of the proposed and reverse antennas. (a) Reflection coefficient (b) Axial Ratio.

of antenna without PCM elements. It means the effective aperture of the antenna is improved. Therefore, the gain of the monopole antenna with PCM coating is enhanced greatly. From the analysis based on the comparison of reflection coefficients and gain, we can see that both of the reflection coefficient and gain of the antenna are improved significantly. It can verify the validity of the proposed structure.

## D. POLARIZATION REVERSE CHARACTERISTIC

The orientation of the PCM element affects the polarization performance of the antenna. By rotating the orientation of the element, the antenna changes from LHCP to RHCP which shows the polarization reverse characteristic. This means the antenna can work in multi-state and provides a great freedom for the practical application. To better understand the influence of the orientation, the proposed and reverse antennas with different orientations as shown in Figure 14 are studied. Figure 15 shows the simulated performance of the two antennas. We can clearly see that the reflection coefficient and axial ratio of the reverse antenna change little compared to the proposed antenna. To better understand the effect of the PCM coating on the polarization transformation, Figure 15(b) shows the axial ratio of the antenna with PCM coating. We can see that the antenna is circularly polarized in operating band ranging from 10.2 GHz to 10.9 GHz. This fully demonstrates that the performance of the two antennas are steady while the polarization characteristic can be changed easily. In Figure 16, it can be clearly seen that the proposed antenna is left-hand circular polarization, and the reverse antenna is right-hand circular polarization. This illustrates that the polarization of the antenna can be reversed by changing the orientation of the PCM element.

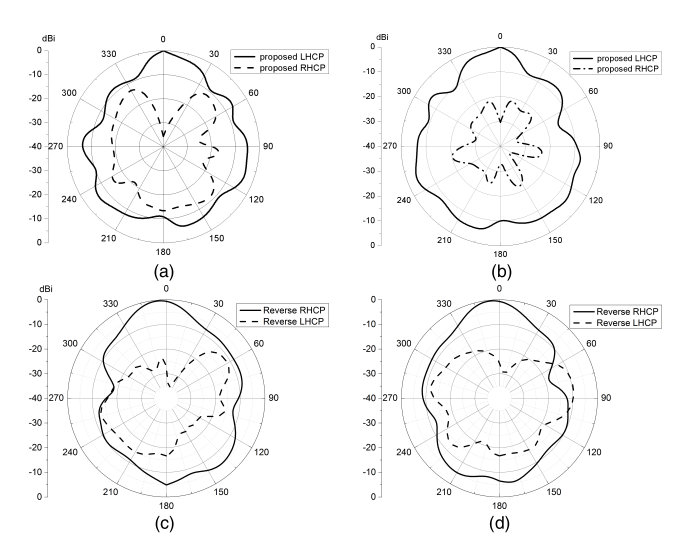


FIGURE 16. Simulated performance of the proposed and reverse antennas. (a) E-plane of proposed antenna (b) H-plane of proposed antenna (c) E-plane of reverse antenna (d) H-plane of reverse antenna.

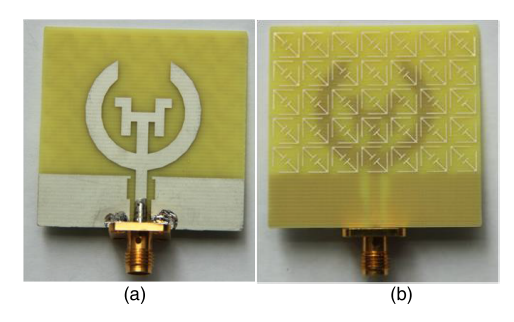


FIGURE 17. Photographs of the proposed antenna. (a) Top view (b) Back view.

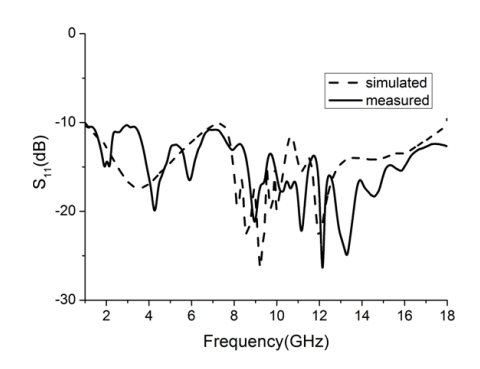


FIGURE 18. Simulated and measured reflection coefficient of the modified antenna.

# III. EXPERIMENTAL RESULTS AND DISCUSSION OF THE PROPOSED ANTENNA

To validate the design, the proposed antenna is fabricated and the prototype in given in Figure 17. The reflection coefficient of the antenna is measured with an AV 3672B vector network analyzer. The simulated and measured reflection coefficients  $(S_{11})$  and the CP axial ratio (AR) are shown in Figure 18 and Figure 19 respectively. We can see that with the PCM coating, the LHCP radiation is achieved in 10.2 to 10.9 GHz. Good

84664 VOLUME 8, 2020



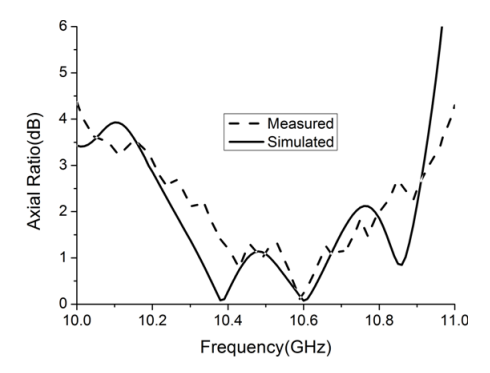


FIGURE 19. Simulated and measured Axial Ratio of the modified antenna.

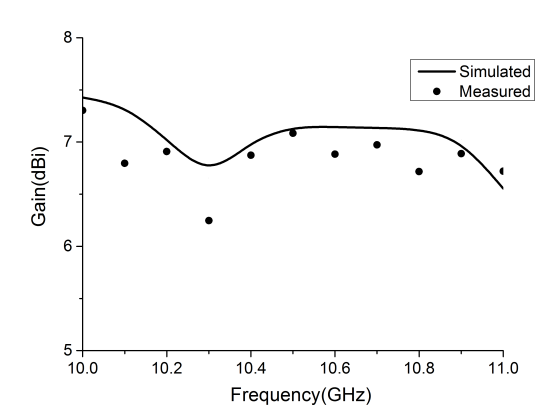


FIGURE 20. Simulated and measured gain of the modified antenna.

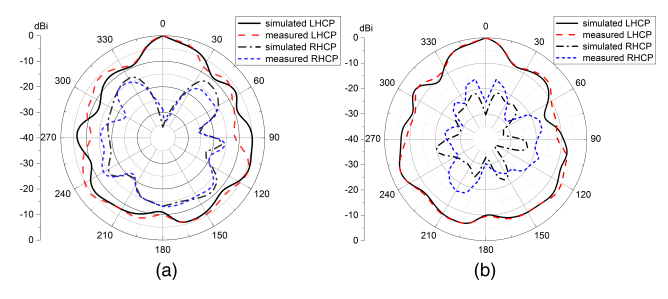


FIGURE 21. Simulated and measured radiation patterns of the proposed antenna at 10.6GHz. (a) E-plane (b) H-plane.

agreement between them can be observed. The measured 10-dB impedance bandwidth is 16.90GHz (1-17.9GHz). And the 3dB AR bandwidths of the proposed antenna are nearly 700MHz (10.2-10.9GHz). We can see that the CP band is valid. The gain and the radiation pattern are measured in an anechoic chamber. The simulated and measured peak gains of the proposed antenna across the working band are shown in Figure 20. We can observe that the gain variation is stable. Finally, Figure 21 (a) and (b) shows the measured radiation patterns of the proposed antenna in the E-plane and H-plane respectively. As shown in the figure, favorable radiation performance and high isolation is realized between the co-and cross-polarized radiations at 10.6GHz.

#### **IV. CONCLUSIONS**

Compact, gain enhanced, and circularly polarized antenna is proposed in this paper. The modified PCM which is made up of a series of arrow-shaped elements distributed partly on the back of the substrate is used as the coating of the antenna. And genetic algorithm (GA) is adopted to obtain the global optimum of the element. By the PCM plane, circularly polarized antenna is obtained with a low profile. The antenna can change from LHCP to RHCP by rotating the orientation of the element. This means the antenna can work in multi-state and provides a great freedom for the practical application. In addition, the gain of the antenna is improved. The measured results are in good agreement with the simulated results. What's more, the simple structure, stable gains, and multi-state of the proposed structure shows a good prospect of application.

#### **REFERENCES**

- M. Ameen and R. K. Chaudhary, "Metamaterial-based wideband circularly polarised antenna with rotated V-shaped metasurface for small satellite applications," *Electron. Lett.*, vol. 55, no. 7, pp. 365–366, Apr. 2019.
- [2] C.-H. Lee, T. V. Hoang, S. W. Chi, S.-G. Lee, and J.-H. Lee, "Low profile quad-beam circularly polarised antenna using transmissive metasurface," *IET Microw., Antennas Propag.*, vol. 13, no. 10, pp. 1690–1698, Aug. 2019.
- [3] H.-P. Li, G.-M. Wang, X.-J. Gao, J.-G. Liang, and H.-S. Hou, "A novel metasurface for dual-mode and dual-band flat high-gain antenna application," *IEEE Trans. Antennas Propag.*, vol. 66, no. 7, pp. 3706–3711, Jul. 2018.
- [4] Y. B. Li, B. G. Cai, Q. Cheng, and T. J. Cui, "Holographic metasurfaces: Isotropic holographic metasurfaces for dual-functional radiations without mutual interferences (Adv. Funct. Mater. 1/2016)," Adv. Funct. Mater., vol. 26, no. 1, p. 155, Jan. 2016.
- [5] H. Li, G. Wang, T. Cai, H. Hou, and W. Guo, "Wideband transparent beamforming metadevice with Amplitude- and phase-controlled metasurface," *Phys. Rev. A, Gen. Phys.*, vol. 11, no. 1, Jan. 2019, Art. no. 014043.
- [6] J. Wang, H. Wong, Z. Ji, and Y. Wu, "Broadband CPW-fed aperture coupled metasurface antenna," *IEEE Antennas Wireless Propag. Lett.*, vol. 18, no. 3, pp. 517–520, Mar. 2019.
- [7] C. Zhang, G. Wang, H. Xu, X. Zhang, and H. Li, "Helicity-dependent multifunctional metasurfaces for full-space wave control," *Adv. Opt. Mater.*, vol. 8, no. 8, Apr. 2020, Art. no. 1901719.
- [8] X.-J. Zou, G.-M. Wang, Y.-W. Wang, and H.-P. Li, "An efficient decoupling network between feeding points for multielement linear arrays," *IEEE Trans. Antennas Propag.*, vol. 67, no. 5, pp. 3101–3108, May 2019.
- [9] J. L. D. S. Paiva, J. P. da Silva, A. L. P. D. S. Campos, and H. D. de Andrade, "Using metasurface structures as signal polarisers in microstrip antennas," *IET Microw., Antennas Propag.*, vol. 13, no. 1, pp. 23–27, Jan. 2019.
- [10] H. Bai, G.-M. Wang, and T. Wu, "High-gain wideband metasurface antenna with low profile," *IEEE Access*, vol. 7, pp. 177266–177273, 2019.
- [11] H. L. Zhu, S. W. Cheung, K. L. Chung, and T. I. Yuk, "Linear-to-Circular polarization conversion using metasurface," *IEEE Trans. Antennas Propag.*, vol. 61, no. 9, pp. 4615–4623, Sep. 2013.
- [12] E. S. R. Montalvão, A. C. P. S. Montalvão, A. L. P. S. Campos, and A. G. Neto, "A new model of metasurface used for linear-to-circular polarization conversion in antenna array," *Microw. Opt. Technol. Lett.*, vol. 58, no. 4, pp. 861–864, Apr. 2016.
- [13] T. Hong, S. Wang, Z. Liu, and S. Gong, "RCS reduction and gain enhancement for the circularly polarized array by polarization conversion metasurface coating," *IEEE Antennas Wireless Propag. Lett.*, vol. 18, no. 1, pp. 167–171, Jan. 2019.
- [14] Y. Li, J. Zhang, S. Qu, J. Wang, L. Zheng, Y. Pang, Z. Xu, and A. Zhang, "Achieving wide-band linear-to-circular polarization conversion using ultra-thin bi-layered metasurfaces," *J. Appl. Phys.*, vol. 117, no. 4, Jan. 2015, Art. no. 044501.

VOLUME 8, 2020 84665



- [15] G. Dong, H. Shi, S. Xia, A. Zhang, Z. Xu, and X. Wei, "Ultra-broadband perfect cross polarization conversion metasurface," *Opt. Commun.*, vol. 365, pp. 108–112, Apr. 2016.
- [16] B. Ratni, A. de Lustrac, G.-P. Piau, and S. N. Burokur, "Electronic control of linear-to-circular polarization conversion using a reconfigurable metasurface," *Appl. Phys. Lett.*, vol. 111, no. 21, Nov. 2017, Art. no. 214101.
- [17] A. Sharma, B. K. Kanaujia, S. Dwari, D. Gangwar, S. Kumar, H. C. Choi, and K. W. Kim, "Wideband high-gain circularly-polarized low RCS dipole antenna with a frequency selective surface," *IEEE Access*, vol. 7, pp. 156592–156602, 2019.
- [18] A. Sharma, D. Gangwar, B. Kumar Kanaujia, S. Dwari, and S. Kumar, "Design of a wideband polarisation conversion metasurface and its application for RCS reduction and gain enhancement of a circularly polarised antenna," *IET Microw., Antennas Propag.*, vol. 13, no. 9, pp. 1427–1437, Jul. 2019.
- [19] Y. Jia, Y. Liu, S. Gong, W. Zhang, and G. Liao, "A low-RCS and high-gain circularly polarized antenna with a low profile," *IEEE Antennas Wireless Propag. Lett.*, vol. 16, pp. 2477–2480, 2017.
- [20] X. Gao, X. Han, W.-P. Cao, H. O. Li, H. F. Ma, and T. J. Cui, "Ultrawideband and high-efficiency linear polarization converter based on double V-Shaped metasurface," *IEEE Trans. Antennas Propag.*, vol. 63, no. 8, pp. 3522–3530, Aug. 2015.
- [21] Y. Liu, K. Li, Y. Jia, Y. Hao, S. Gong, and Y. J. Guo, "Wideband RCS reduction of a slot array antenna using polarization conversion metasurfaces," *IEEE Trans. Antennas Propag.*, vol. 64, no. 1, pp. 326–331, Ian 2016
- [22] A. J. Kerkhoff and H. Ling, "Design of a band-notched planar monopole antenna using genetic algorithm optimization," *IEEE Trans. Antennas Propag.*, vol. 55, no. 3, pp. 604–610, Mar. 2007.
- [23] J.-R. Qi, Y. Dang, P.-Y. Zhang, H.-T. Chou, and H.-S. Ju, "Dual-band circular-polarization horn antenna with completely inhomogeneous corrugations," *IEEE Antennas Wireless Propag. Lett.*, vol. 19, no. 5, pp. 751–755, May 2020.



**TING WU** was born in China, in 1987. She received the B.S. and Ph.D. degrees in electromagnetic field and microwave technology from Xidian University, Xi'an, China, in 2009 and 2016, respectively. She is currently working with the Xi'an University of Technology. Her research interests include antenna array and metasurfaces.



**JUAN CHEN** was born in China, in 1987. She received the Ph.D. degree in circuits and systems technology from the Xi'an University of Technology, China, in 2016. She is currently working with the Xi'an University of Technology. Her research interest is optical communication technology.



**MING-JUN WANG** was born in China, in 1979. He is currently a Professor and a Supervisor of a Ph.D. student. His research interests are broadly in the areas of the electromagnetic (light) scattering from the rough surface, complex targets and its applications, which include electromagnetic (light) scattering, electromagnetic theory, and statistical optics.

. . .

84666 VOLUME 8, 2020